Thermal Diffusion of Salt Solutions in Single-Stage Cells and in Continuous Horizontal Columns: the System Copper Sulfate - Cobalt Sulfate - Water

G. T. FISHER, JOHN W. PRADOS, and L. P. BOSANQUET

The University of Tennessee, Knoxville, Tennessee

The application of thermal diffusion to the separation of a pair of salts in aqueous solution was investigated. Experiments were conducted with the system copper sulfate-cobalt sulfate-water with both static, single-stage cells and continuous, countercurrent flow contactors (or columns) of the horizontal Jury-Von Halle type which utilizes flow through a porous membrane. Design equations for the continuous columns were developed, based on an idealized representation of the combined hydrodynamic and diffusion problem. Data from the single-stage experiments were used in conjunction with these equations to predict stage separation factors and transfer unit heights. These mass transfer parameters were measured under various operating conditions on continuous units of two different sizes.

The effects of size and operating conditions on the separation factor and transfer unit height were successfully predicted by use of the design equations. The accurate calculation of these quantities directly from single-stage separation data was less successful, owing to the highly idealized nature of the mathematical model employed.

Homogenous solutions when subjected to a strong temperature gradient exhibit a tendency toward separation along the gradient. This effect, known as "thermal diffusion," is usually quite small but can be multiplied by use of continuous countercurrent contacting equipment to produce practical separations (*1*). Thermal diffusion offers attractive possibilities for carrying out difficult separations and can be used effectively to separate such systems as isotopic mixtures and optical isomers. However the technique is rarely applied commercially owing to high heat and equipment costs which make the process uneconomical for all except separations that are very costly to effect by other means and a general lack of understanding of the phenomenon, particularly in the liquid phase, which precludes rational equipment design without an extensive development program for each system of interest.

The overall aim of the investigation has been to develop methods for carrying out thermal diffusion separations of metallic elements in aqueous solutions of their salts and for estimating separation costs; it was hoped that the technique might eventually be applied to the purification of certain metals that are difficult to separate from contaminants in their ores.

The specific avenues of attack on this problem have been as follows:

1. The design and construction of a continuous countercurrent thermal diffusion contactor or column of the horizontal Jury-Von Halle type (*2*).
2. Operation of this column with a convenient aqueous two-salt system and evaluation of performance and determination of the effects of operating conditions on the mass transfer parameters.
3. Studies of static single-stage separations in a number of aqueous two-salt systems (results expressed as Soret coefficients for the system) and use of these results in conjunction with column operating data to develop methods for estimating equipment size requirements from Soret coefficient data.
4. Analysis of the above results to attempt to develop a better understanding of the process of thermal diffusion in aqueous salt solutions and hence provide a firmer basis for design and scale-up procedures.

G. T. Fisher is at Vanderbilt University, Nashville, Tennessee. L. P. Bosanquet is with Monsanto Chemical Company, St. Louis, Missouri.

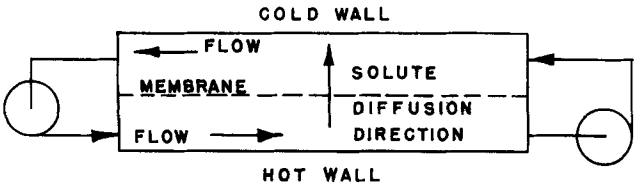

Fig. 1. Schematic representation of a Jury-Von Halle horizontal thermal diffusion column.

The historical background of thermal diffusion is given by Powers and Wilke (*1*). Extensive experimental studies of salt solutions in Soret cells (static single-stage contacting devices) have been reported by Soret (*3*); Chapman, Tyrrell, and Wilson (*4*); Chipman (*5*); Tanner (*6*), (*7*); Tyrrell (*8*), Alexander (*9*), (*10*); and Chanu and Lenoble (*11*), (*12*). The separation of electrolyte solutions in columns of the thermogravitational (Clusius-Dickel) design has been investigated extensively by Hirota (*13*), (*14*), (*15*) and others.

The unique continuous separation equipment used by the authors was first described by Von Halle and Jury (*2*). Their device, which does not employ thermal convection currents to induce the bulk flow, creates two flow channels by the use of a porous membrane, such as cellophane. Each channel, as shown in Figure 1, is bounded by a heat transfer surface and the membrane, together with appropriate side walls. Entrance and exit lines are placed at each end, and the solution is pumped through the channels by external pumps. Thermal diffusion takes place through the membrane. The column is operated in a horizontal position to prevent density gradients from causing bulk flow inside a channel as in the vertical Clusius-Dickel column. The advantages of this device are that the bulk flows can be controlled externally and independently of the temperature gradient or the spacing between the walls, and that any system which exhibits the Soret effect can be separated continuously. Another advantage is that narrow and extremely uniform wall spacing is not essential, as is necessary in the vertical Clusius-Dickel column.

A review of existing data on Soret coefficients of salt solutions indicated a need for an apparatus design that would give reproducible results for systems containing two or more salts in water. It was deemed essential to have reproducible Soret coefficient data in order to analyze accurately the operation of the continuous device. The system chosen for study was the copper sulfate-cobalt sulfate-water system, with initial solution concentrations of 0.4 to 0.5 molar in each salt. This system was chosen because of ease of analysis by spectrophotometric methods and because of the known Soret effects of each individual salt.

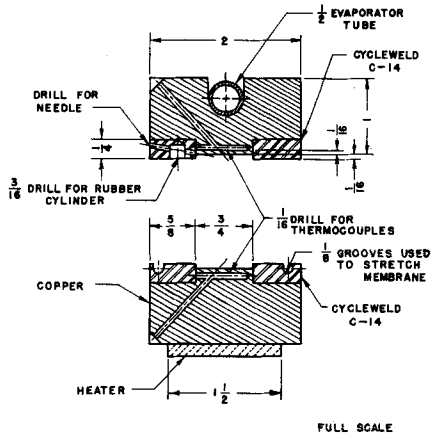

Fig. 2. Cross-sectional view of the small column.

EXPERIMENTAL EQUIPMENT AND PROCEDURE

Equipment

Two thermal diffusion columns and one Soret cell were used; the large column had a diffusion area of 0.915 sq.ft., and the small column 0.106 sq.ft. The Soret cell had an area of 0.0323 sq.ft. and a volume of 30 ml.

The Small Column. The small column was constructed from two copper bars, each 24 × 2 × 1 in. The top bar, as it was operated, was milled longitudinally to receive a 1/2-in. copper tube, which was soldered to the bar and carried the refrigerant. A 1-3/4- × 22-in. Chromalox 1,500-w. electric strip heater was fastened to the bottom bar with screws. Figure 2 shows a detailed cross section of the column. A 3/16 in. deep × 5/8 in. wide shoulder was machined completely around each bar on the side opposite the thermal sources; a plastic strip 1/4 in. deep × 5/8 in. wide was placed on this shoulder. The plastic surface extended 1/16 in. beyond the surface of the copper bar; this 3/4 in. wide × 1/16 in. deep depression formed three of the four walls of the column flow channel and the two ends. A cellophane membrane stretched over the depression formed the fourth wall of the flow channel. Parallel to the flow channel surface 1/16 in. away, three holes of 1/16-in. diameter were drilled for thermocouple wires; holes were drilled through the copper bar for access to these thermocouple wells. In each end of each bar 1/16-in. holes were drilled through the bar to the center of the channel for flow entry; external fittings were made for connection of 1/16-in. I.D. flexible tubing. The two halves of the column were clamped together with a cellophane membrane between the two halves. The top bar was wrapped in a commercial refrigeration insulation tape to reduce the heat load and condensation of atmospheric moisture.

The plastic used to form the side walls was a combination of layers of Cycleweld C-17 and Cycleweld C-14, both resin products. The C-17 was used next to the hot-side bar because of its better strength properties, particularly at high temperatures. The C-14 was used because it sets more slowly after pouring than C-17, and is easier to work with. As shown in Figure 2, slots were machined in the Cycleweld on the bottom half to take two 1/8-in. Monel welding rods which were 1/2 in. longer than the copper bar. A cellophane membrane 2 in. wide with a 2 in. wide Teflon gasket on each side was stretched between the Monel rods; the Teflon gasket had a hole, 20-1/4 in. × 3/4 in. (area 0.106 sq. ft.), cut in the center. These gaskets were necessary to prevent failure of the cellophane at the end where the cold stream entered the channel; the brittleness of cellophane at low temperatures created the need for the gaskets. Further discussion of the need for the Teflon gaskets is given by Fisher (*16*).

The Large Column. The large thermal diffusion column was constructed from two silicon bronze (95% copper, 4% silicon, and 1% manganese) plates, each 17 × 17 × 1/2 in., mounted in a press constructed from 18 × 24 × 2 in. steel plates, with a network of refrigerant channels in one plate and ten 5/8 × 16-in. cartridge heaters inserted in drilled holes in the other. This was the same press as used by Von Halle and Jury (*2*), with only one modification; on the lower plate, which moved on 1-in. diameter steel guides, the steel bushings were replaced with special Bakelite bushings. Each silicon bronze plate was machined flat and a 1/8-in. cork sheet glued on with clear varnish. Twenty flow channels, 14-5/8 × 1/2 in., were cut in the sheet cork and alternate ends connected to form one continuous channel. The two plates were placed together with a sheet of 17- × 17-in. cellophane between them. The detailed layout is shown in Figure 3. This geometry gave a contact area of 1.020 sq. ft.; because of the impervious Teflon covers used over the end channels to prevent membrane failure only 0.915 sq. ft. was available for diffusion. Entrance ports and sample ports were constructed as shown in Figure 3. Machined Everdure (silicon bronze) screws were used to provide connections for 1/16-in. I.D. Tygon tubing. Because of corrosion problems the screw in the hot-side entrance port had to be replaced with a Lucite screw. The 3/32-in. sample ports shown were plugged

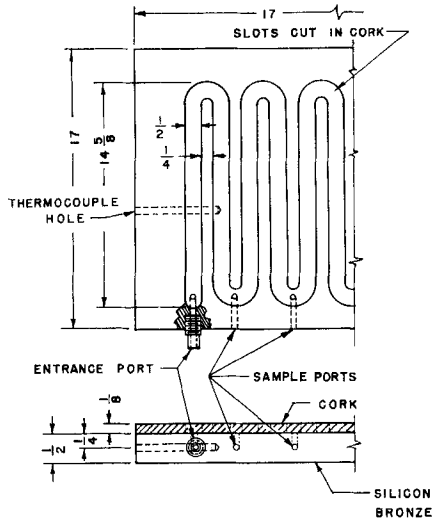

Fig. 3. Layout of plates used in the large column.

with 3/32-in. Teflon rods. Thermocouple holes were drilled 2 in. into the plates, as shown.

The Soret Cell. The Soret cell was similar in construction to the small continuous column. It was heated by two 3/8- × 6-in. Chromalox 250-w. cartridge heaters inserted in the top bar and cooled by a 1/2-in. refrigeration tube drilled in the bottom bar. The copper bars were 2 × 8 × 1 in. The chamber formed by the Cycleweld and each copper bar was 0.197 in. (1/2 cm.) deep by 5.90 × 0.787 in. (15 × 2 cm.). The Cycleweld was coated on the inside of the chamber with Eastman-910 cement to stop displacement of air from small pockets in the walls. A Formica rib 0.180 in. high was inserted as a central support for the cellophane membrane that was stretched between the two chambers. Each chamber had a filling port and a venting port. These insured equal pressure on each side of the membrane, complete removal of air from the cell, and complete removal of the chamber liquid volumes for analysis. This cell was operated with the hot side on top to minimize the chance of any convection currents. Complete details of this system are given by Bosanquet (*17*).

Auxiliary Equipment

Each piece of equipment was heated electrically. As an electromotive force is developed by the differences in temperature and concentration of the salt solution, care was taken to insulate electrically the hot side of any diffusion device from the cold side. Because of inherent grounds in the cold-side refrigeration systems, and ground in the power source, an isolation transformer was placed between the power source and the heaters. Variacs were used to provide variable heat inputs. Refrigeration was provided by Freon-12 compressor-condenser systems. Expansion valves with superheat control were used for throttling, and evaporator pressure regulators were used to hold the pressure inside each unit constant. Gauges indicated evaporator pressures.

The flow of solution in the continuous columns was induced by Sigmamotor pumps (finger pumps) operating with 1/16-in. I.D. × 1/16-in. wall Tygon tubing. The pumps lifted the solution from a reservoir to a constant head tank. The solution then flowed by gravity through the column and into a standpipe. The overflow from the standpipe was returned to the reservoirs. This arrangement is shown in Figure 4. The head tanks operated with a holdup volume of 5 to 10 ml., and the liquid surface was 1 to 2 in. above the standpipe level. The levels of the standpipe exits from both channels were the same. The head tanks were 2 ft. above the level of the column; hence the columns were under a positive pressure in slight excess of 2 ft. of water. The levels of the two reservoirs were arranged so that any product from one end of the column flowed by gravity back into the other reservoir; hence the system operated as a completely closed system.

Temperatures were measured with iron-constantan thermocouples and were recorded on multipoint strip-chart recorders. Readings were checked periodically with a portable precision potentiometer.

Procedure

Continuous Column Operation. The continuous columns were operated in a horizontal position, with the cold wall on top, as shown in Figure 1. They were operated with countercurrent flow for all runs. The flow through each channel was controlled by changing the input rate to the small vented head tank; the level in this tube was allowed to change until the output rate was equal to the input rate. The flow rates on the small column were varied from 2 to 10 ml./hr. and on the large column from 10 to 35 ml./hr. The flow rates into the column were measured by connecting the pump input lines to 50-ml. burettes and measuring the time-volume relation; the outputs of the column were measured by allowing the overflow of the standpipes to drain into 50-ml. burettes. The product rate was measured by isolating the two reservoirs and allowing the small burette reservoir to fill. At least 12 ml. of each solution was caught in each measurement.

The transient start-up time of the system was quite long; at the lowest flow rates the small column took 21 days to come to a steady state. This problem was circumvented to some degree however by placing a dilute solution in the cold-side feed reservoir and allowing the system to come to steady state from an over separated condition rather than from a condition of no separation. Runs of 2 to 4 days length could be completed in this manner. The small reservoirs were operated with 5- to 10-ml. holdup and the large reservoirs with 7 liters.

The small column was operated with temperatures of 38° to 40°F. on the cold side and 142° to 148°F. on the hot side. The large column was operated at 52°F. on the cold side and 122°F. on the hot side. These temperatures were measured within the plates, and when corrected to yield true surface values they gave wall-to-wall temperature differences of 100°F. in the small column and 60°F. in the large column. The small column heater consumed 350 w., the large column heater 1,060 w.

Solution samples for chemical analyses were withdrawn from the overflow from the standpipes; this allowed direct products of the column to be analyzed without disturbing its operation.

Several runs were performed without shutting down the columns; after a column was ascertained to be at steady state, only the flow rates were changed.

During start-up of the large column on unexplained transient separation of considerable magnitude was observed, in the direction opposite to that observed at steady state. This phenomenon has been described in detail by Fisher (*16*). It did not occur when operating conditions were changed but only when the column had been cleaned and started up with fresh solution.

Soret Cell Operation. The Soret cell operation is essentially restricted to filling and emptying the cell. A PD-600 cellophane membrane presoaked in distilled water was partially dried and put in place. The cell was then clamped together and slightly inclined. Each section of the cell was filled with a hypodermic syringe and needle from the bottom, while the air was allowed to vent to the top. This enabled the amounts of solution inserted and removed in a similar manner to be measured accu-

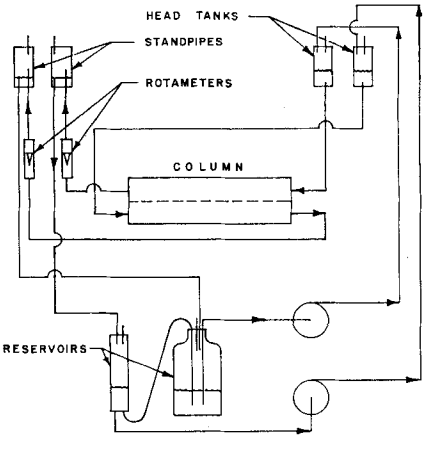

Fig. 4. Schematic of the flow system.

rately. The run lengths varied from 29 to 84 hr., but a run length of 29 hr. was found to be sufficient to attain equilibrium. (This is not a ture thermodynamic equilibrium, as a temperature gradient must exist even when the net mass transfer rate has vanished.) After this period the entire solution was removed from both sides and analyzed.

Analytical Method. All solutions were chemically analyzed with a DU spectrophotometer at 525- and 700-mμ wavelengths. The Lambert-Beer law was used with the assumption of additive absorbancies of the two salts in solution.

THEORY

The rate expression in this work is that given by Grew and Ibbs (*18*) for the net diffusion rate effected by simultaneous temperature and concentration gradients*

$$J_A = \rho\left[-\mathcal{D}'\,\xi\,(1-\xi)\,\frac{\partial T}{\partial r} - \mathcal{D}\,\frac{\partial \xi}{\partial r}\right] \qquad (1)$$

For dilute solutions the quantity $(1 - \xi) \cong 1$, and this approximation will be used in the present work, as the theory is not applied to any operations in which ξ is greater than 0.01. The approximation that all physical properties and constants, including density and viscosity, are independent of temperature and composition will also be used.

The Soret Cell

In a Soret cell a concentration gradient and a thermal gradient are established between two parallel walls which are respectively heated and cooled. At steady state there is no net mass transfer from one part of the system to another; hence $J_A = 0$. If in Equation (1) J_A is equated to zero, then one may integrate to obtain

$$\xi = \xi_1\, e^{-\sigma(T-T_1)} \qquad (2)$$

where the quantity $\mathcal{D}'/\mathcal{D} = \sigma$ is defined as the Soret coefficient. If one considers the cell as consisting of two regions separated by a membrane, then a material balance on the cold side is

$$A\bar{\xi}_1 \rho a = \int_o^a A\xi\rho dr \qquad (3)$$

If the thermal conductivity of the solution remains nearly constant, the temperature profile across the cell should be linear. Using this assumption and the assumption of negligible temperature drop in the membrane one obtains

$$\bar{\xi}_1 = \frac{2\xi_1 e^{\sigma T_1}}{-\sigma[T_2 - T_1]}\left[e^{\frac{-\sigma(T_1+T_2)}{2}} - e^{-\sigma T_1}\right] \qquad (4)$$

A similar analysis can be performed for $\bar{\xi}_2$. The ratio is then

$$\frac{\bar{\xi}_2}{\bar{\xi}_1} = e^{\frac{-\sigma(T_1-T_2)}{2}} \qquad (5)$$

Equation (5) permits calculation of Soret coefficients from temperature and mean concentrations alone.

Continuous Column

If the temperature gradient $\tau_M = (\partial T)/(\partial l)$ and the rate of diffusion J_o for unidirectional heat transfer and diffusion across the membrane are considered constant, the variables in Equation (1) may be separated into the equation

$$\frac{d\xi}{-\frac{J_o}{\rho\phi\mathcal{D}} + \sigma\,\tau_M\,\xi} = dl \qquad (6)$$

If Equation (6) is integrated between the limits of $\xi(l = 0) = \xi_o$ and $\xi(l = \delta) = \xi_o'$, one obtains by solving for J_o

$$J_o = \frac{\sigma\tau_M\mathcal{D}\phi\rho}{(1 - e^{\sigma T_M\delta})}\,(\xi_o' - \xi_o\, e^{\sigma T_M\delta}) \qquad (7)$$

The rate of diffusion was derived on the assumption that the membrane has no effect on diffusion except to reduce the free area by the quantity ϕ. If the system is operated with $J_o = 0$, that is as a Soret cell with no net diffusion, Equation (7) gives

$$\xi_o' = \xi_o\, e^{\sigma\tau_M\delta} \equiv \xi_o'^* \qquad (8)$$

When one uses Equation (8), Equation (7) becomes

$$J_o = \frac{\sigma\tau_M\mathcal{D}\phi\rho}{(1 - e^{\sigma\tau_M\delta})}\,(\xi_o' - \xi_o'^*) \qquad (9)$$

In conventional mass transfer terminology Equation (9) states that the rate of diffusion is proportional to the difference between the concentration on one side of the membrane and an equilibrium concentration.

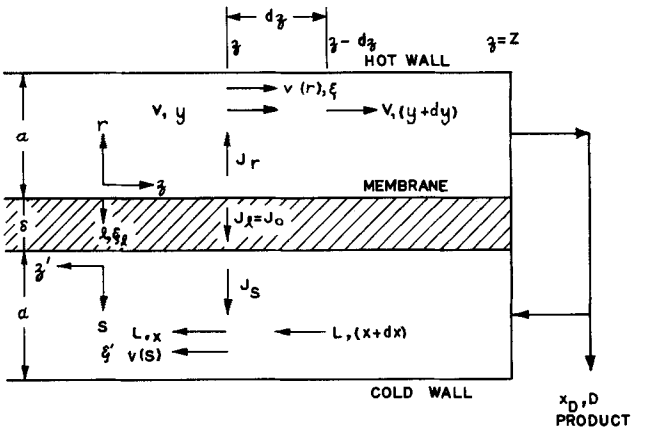

Fig. 5. Schematic of the cross section of a column.

If a column is operated as shown in Figure 5 with a product withdrawal rate, D moles/time, of composition x_D, then a material balance on the product end of the column gives

$$Vy = L\,x + Dx_D \qquad (10)$$

$$V = L + D \qquad (11)$$

A material balance on a section of differential length dz yields, under the assumption of no longitudinal diffusion in the membrane

$$J_o = -\frac{L}{b}\frac{dx}{dz} = -\frac{V}{b}\frac{dy}{dz} \qquad (12)$$

The diffusion Equation (12) and the material balance Equation (10) may be solved simultaneously from either of two assumptions: that complete mixing takes place on either side of the membrane, or that no mixing takes place.

* For electrolytes a term giving the contribution of any electrical potential gradient to the net flux should be included in Equation (1). Such a term has been included by Guthrie et al. (*19*) in treating the special case of zero net flux. However the effect is quite difficult to evaluate in general, and since the work of Bosanquet (*17*) appears to indicate that its effect is quite small, it has not been included here.

The actual operating condition of a column would be expected to lie between these two limiting cases.

If perfect mixing in the individual channels is assumed, then

$$x = \xi' = \xi_o', y = \xi = \xi_o, x^* = \xi_o'^* = \xi'^* \tag{13}$$

and Equation (9) becomes

$$J_o = k_L' (x^* - x) \tag{14}$$

where

$$k_L' \equiv \frac{\sigma\tau_M \mathcal{D} \phi \rho}{e^{\sigma\tau_M\delta} - 1} \tag{15}$$

By combining Equations (8) and (13) one obtains

$$K' x^* = y \tag{16}$$

where

$$K' \equiv e^{-\sigma\tau_M\delta} \cong e^{-\sigma\Delta T} \tag{17}$$

The approximate relation is valid if the entire temperature difference is developed across the membrane, as it would be with perfect mixing.

It will be noted that k_L' has the significance of a mass transfer coefficient, while K' acts as a phase equilibrium constant.

If no mixing is assumed, the solution to the equations of viscous flow for a constant viscosity fluid between two parallel plates of infinite width is

$$v(r) = \frac{6V}{a^3 b \rho} (ar - r^2) \tag{18}$$

This situation is approximated in the columns, as the channel width is large compared with the vertical depth. If longitudinal diffusion is neglected, then the transport relations are

$$J_r = \rho \left[-\mathcal{D}' \xi_\tau - \mathcal{D} \frac{\partial \xi}{\partial r} \right] \tag{19}$$

$$J_z = \rho v \xi \tag{20}$$

The continuity equation at steady state is

$$\frac{\partial(\rho\xi)}{\partial t} = 0 = -\operatorname{div} \vec{J} = -\frac{\partial J_r}{\partial x} - \frac{\partial J_z}{\partial z} \tag{21}$$

A combination of the transport Equations (19) and (20) and the continuity Equation (21) yields

$$\frac{\partial}{\partial r} J_r + \frac{\partial}{\partial z} (\rho v \xi) = 0 = \frac{\partial}{\partial r} \rho \left[-\mathcal{D}' \xi_\tau - \mathcal{D} \frac{\partial \xi}{\partial r} \right] + \frac{\partial}{\partial z} (\rho v \xi) \tag{22}$$

The boundary conditions are

$$\begin{aligned} J_r(0) &= -J_o & \xi(r, 0) &= x_F \\ J_r(a) &= 0 & \int_0^a b \rho v \xi(r, Z)\, dr &= x_D V \end{aligned} \tag{23}$$

The formulation of the problem in the other half channel yields an identical differential equation and boundary conditions. If one assumes that the flow rates L and V are constant throughout the column, and that $(\partial\xi)/(\partial z) = (dy)/(dz)$ at any given z, the variables are separable, and one obtains by a first integration of Equation (22)

$$\frac{1}{\rho} \int_r^a d(J_r) = -\int_r^a v \frac{dy}{dz} dr \tag{24}$$

From the boundary conditions of Equation (23) this becomes

$$\frac{1}{\rho} [J_r(a) - J_r(r)] = \frac{-J_r}{\rho} = -\sigma \mathcal{D} \xi_\tau - \mathcal{D} \frac{d\xi}{dr} = \int_r^a v \frac{dy}{dz} dr \tag{25}$$

By use of the integrating factor $e^{\sigma\tau r}$ this first-order linear differential equation can be integrated, and one obtains

$$\int_0^r d(e^{\sigma\tau r}\xi) = \int_0^r \left[\frac{d\xi}{dr} + \sigma \xi_\tau \right] e^{\sigma\tau r} dr = -\frac{1}{\mathcal{D}} \frac{dy}{dz} \int_0^r e^{\sigma\tau r} dr \int_r^a v\, dr \tag{26}$$

or

$$\xi(r) = \xi_o e^{-\sigma\tau r} - \frac{e^{-\sigma\tau r}}{\mathcal{D}} \frac{dy}{dz} \int_0^r e^{\sigma\tau r} dr \int_r^a v\, dr \tag{27}$$

The total flow in the z direction is

$$Vy = \int_0^a \rho b v(r) \xi(r) dr \tag{28}$$

If Equation (27) is substituted into Equation (28) one obtains

$$y = \frac{\rho b \xi_o}{V} \int_0^a v e^{-\sigma\tau r} dr - \frac{\rho b}{\mathcal{D} V} \frac{dy}{dz} \int_0^a v e^{-\sigma\tau r} dr \int_0^r e^{\sigma\tau r} dr \int_r^a v\, dr \tag{29}$$

The integrals can be evaluated with the velocity distribution of Equation (18), whereby one obtains

$$y = \xi_o f_1(c) - \frac{V}{\sigma\tau b \rho \mathcal{D}} \frac{dy}{dz} f_2(c) \tag{30}$$

and

$$x = \xi_o' f_1(c') + \frac{L}{\sigma\tau' b \rho \mathcal{D}} \frac{dx}{dz} f_2(c') \tag{31}$$

where

$$c = \sigma\tau a = -\sigma\tau' a = -c' \tag{32}$$

$$f_1(c) = \frac{6}{c^3} [e^{-c}(c + 2) + (c - 2)] \tag{33}$$

$$f_2(c) = \frac{36}{c^3} \left\{ 4[e^{-c}(1 + c) - 1] + c^2(e^{-c} + 1) - \frac{1}{3} c^3 e^{-c} - \frac{c^4}{6}(e^{-c} + 1) + \frac{c^5}{30} + \frac{c^6}{72} \right\} \tag{34}$$

If the maximum value of c is such that the approximation $e^c \cong 1 + c$ is valid, then

$$f_2(c) \cong 0.3714c - 0.1250c^2 - 0.0529c^3 \tag{35}$$

Equations (7), (12), (30), and (31) may be combined to give

$$J_o = \frac{\sigma \mathcal{D} \rho}{\left[\frac{1 - e^{\sigma\tau_M\delta}}{\tau_M \phi} + \frac{f_2(-c)}{\tau f_1(-c)} - \frac{f_2(c) e^{\sigma\tau_M\delta}}{\tau f_1(c)} \right] \times \left[\frac{x}{f_1(-c)} - \frac{y e^{\sigma\tau_M\delta}}{f_1(c)} \right]} \tag{36}$$

If the composition x^* is defined as the average cold-channel concentration in equilibrium with the average hot-channel concentration y, that is when $J_o = 0$, then Equation (36) gives

$$x^* = \frac{y f_1(-c)}{f_1(c)} e^{\sigma\tau_M\delta} \equiv \frac{1}{K''} y \tag{37}$$

Equation (36) then becomes

$$J_o = k_L'' (x^* - x) \tag{38}$$

where

$$k_L'' \equiv \frac{\sigma \mathcal{D} \rho \tau_M}{\left[(e^{\sigma\tau_M\delta} - 1) \frac{f_1(-c)}{\phi} - \frac{\tau_M f_2(-c)}{\tau} + \frac{\tau_M}{\tau} \frac{f_1(-c)}{f_1(c)} f_2(c) e^{\sigma\tau_M\delta} \right]} \quad (39)$$

The ratio $\frac{f_1(c)}{f_1(-c)}$ can be shown to be

$$\frac{f_1(c)}{f_1(-c)} = e^{-c} = e^{-\sigma\tau a} \quad (40)$$

Therefore K'' is given by

$$K'' = e^{-\sigma(\tau_M\delta + \tau a)} \cong e^{\frac{-\sigma\Delta T}{2}} \quad (41)$$

The approximate relation is valid if the temperature drop across the membrane is small compared with the temperature drop in one of the channels.

By combining the material balance Equations (10) and (11) with Equation (12) and the general form of either Equation (14) or (38), one has

$$-\frac{L}{b}\frac{dx}{dz} = k_L \left[\left(\frac{L}{KV} - 1 \right) x + \frac{D}{KV} x_D \right] \quad (42)$$

The values of k_L and K depend on the model chosen; that is $k_L = k_L'$ and $K = K'$ for the complete mixing model, and $k_L = k_L''$ and $K = K''$ for the laminar flow model. If one defines the height of a transfer unit based on the cold stream as

$$h_L \equiv \frac{L}{bk_L} \quad (43)$$

then one can obtain by integration of Equation (42)

$$\frac{x}{x_D} = \frac{1}{K(R+1) - R} \times \left\{ 1 - (R+1)(1-K) e^{\left[\frac{R}{K(R+1)} - 1 \right] \frac{Z-z}{h_L}} \right\} \quad (44)$$

where R is the reflux ratio, $R = L/D$, and Z is the total length of the column. At total reflux this equation reduces to

$$\frac{x}{x_D} = e^{\left(\frac{1}{K} - 1 \right) \frac{Z-z}{h_L}} \quad (45)$$

These developments are for a single component in a dilute solution. The equations should apply equally well in describing the separation of each of several solutes from a solvent, provided that the presence of the additional components does not affect the binary diffusion coefficients between solute and solvent. To describe the separation of one solute relative to another, it is convenient to introduce the separation factor α. For the separation of salt I relative to salt II, α is given by

$$\alpha \equiv \frac{\left(\frac{y}{x^*}\right)_I}{\left(\frac{y}{x^*}\right)_{II}} = \frac{K_I}{K_{II}} \quad (46)$$

Table 1*a*. Soret Coefficients of Single Salt Solutions

Solute	Initial molarity	Average temperature difference, °C.	Mean temperature, °C.	Soret coefficient, °C.$^{-1}$
$CuSO_4$	0.480	28.4	32.8	8.35×10^{-3}
$CoSO_4$	0.476	27.8	32.2	5.95×10^{-3}

Table 1*b*. Soret Coefficients of Two Salt Solutions

Solute	Initial molarity	Average temperature difference, °C.	Mean temperature, °C.	Soret coefficient, °C.$^{-1}$
$CuSO_4$	0.452	27.8	32.2	7.65×10^{-3}
$CoSO_4$	0.454			5.38×10^{-3}
$CuSO_4$	0.452	22.2	26.7	7.18×10^{-3}
$CoSO_4$	0.454			4.85×10^{-3}
$CuSO_4$	0.452	16.7	21.1	5.83×10^{-3}
$CoSO_4$	0.454			3.69×10^{-3}

EXPERIMENTAL RESULTS

Soret Coefficients

The average values of the Soret coefficients of single-salt solutions are given in Table 1*a*. Corresponding values of the Soret coefficients in two salt solutions are given in Table 1*b*. The probable error in all cases is between 1.0 and 2.1%. The determinations in each case represent the average of four runs except the two runs with a smaller temperature difference which are given in the last two lines of Table 1*b*; these data are from single runs only. The theory of Guthrie et al. (*19*) predicts that in a two salt mixture the Soret coefficient of one salt should increase and the other decrease. These data do not appear to support the theory, as the Soret coefficients of both salts decrease slightly in each other's presence. A trial-and-error fit of Soret coefficient vs. temperature with an electronic analogue computer gave for copper sulfate

$$\sigma = 4.00 \times 10^{-3} + 0.116 \times 10^{-3} T$$

and for cobalt sulfate

$$\sigma = 2.00 \times 10^{-3} + 0.110 \times 10^{-3} T$$

σ in °C^{-1}, T in °C

These equations provided the best linear fit to the three sets of data points.

Continuous Column Parameters

The small column was operated at total reflux and flow rates between 2 and 10 ml./hr. Equation (45) predicts

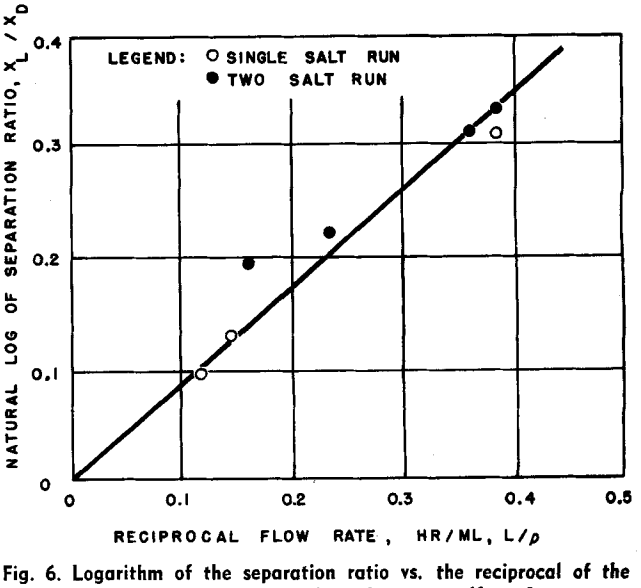

Fig. 6. Logarithm of the separation ratio vs. the reciprocal of the flow rate for total reflux separation of copper sulfate from water.

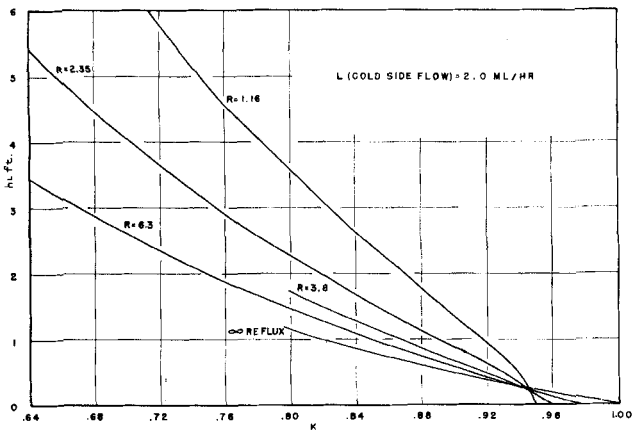

Fig. 7. Determination of the small column separation parameters for copper sulfate.

that a plot of log x_L/x_D vs. ρ/L should be a straight line, if h_L is proportional to the flow rate. Figure 6 is such a plot for the separation of the copper sulfate. Equation (43) indicates that h_L is proportional to the flow rate (for a given column where the channel width b is fixed) if the mass transfer coefficient k_L is constant. Equations (15) and (39) indicate that the mass transfer coefficient is a function only of the temperature gradients, channel dimensions, and properties of the system. Figure 6 supports the predictions of these equations that the height of the transfer unit is directly proportional to the flow rate in a given column for a particular wall-to-wall temperature difference.

If two runs are made with the same wall-to-wall temperature differences and same cold-side flow rate L, then the heights of the transfer unit for the two runs should be the same. As the reflux ratio of the two runs could be changed by changing the hot-side flow rate only, two runs should determine a unique value of h_L and K through Equation (44). Also any number of runs with the same cold-side flow rate should all have a common and unique value of h_L and K. Figure 7 is the plot of the locus of (h_L, K) for each of five runs, all with a common cold side flow rate of 2 ml./hr. The values of h_L and K for this flow rate are determined by the common intersection point.

In Table 2 the observed values of h_L and K for a cold-side flow of 2 ml./hr. are compared with those predicted by the theoretical Equations, (15), (17), (39), (41), and (43). Parameters in these equations were obtained from the literature where available. Soret coefficients σ were those reported above, and membrane free areas ϕ were as given by Couch (*20*). K_{mix} and h_{L-mix} are values predicted by Equations (15) and (17) for complete mixing in each channel; K_{lam} and h_{L-lam} are values predicted by Equations (39) and (41) for laminar flow with a parabolic velocity profile. Data on a total of twenty-one runs have been tabulated and analyzed by Fisher (*16*).

The data of Figure 7 uniquely determine (h_L, K); these values are not in the region of expected intersection for either of the theories. Neither is the intersection in a region that would be expected from a logical combination of these two theories.

In order to test the validity of the developed equations for design and scale-up calculations values of K and h_L were calculated for the large column from Equations (39) and (41), based on operating data for the small column. These values are designated $K_{scale\text{-}up}$ and $h_{Lscale\text{-}up}$ and are based on a large-column flow rate of 16.1 ml./hr. The values actually observed for this flow rate from the large column are also reported. The agreement between calculated and observed values is within 5% for all cases, indicating that the equations do give the correct dependence of separation parameters on flow rate, temperature difference and channel dimensions.

Table 2. Separation Parameters of the Small Column

Salt	K_{mix}	K_{lam}	K_{obs}	$h_{L\text{-}mix}$, ft.	$h_{L\text{-}lam}$, ft.	$h_{L\text{-}obs}$, ft.
(1)	(2)	(3)	(4)	(5)	(6)	(7)
$CuSO_4$	0.68	0.82	0.944	0.59	0.91	0.26
$CoSO_4$	0.74	0.86	0.962	0.56	0.78	0.24

Table 3. Separation Parameters of the Large Column

Salt	K_{obs}	$K_{scale\text{-}up}$	$h_{L\text{-}obs}$, ft.	$h_{L\text{-}scale\text{-}up}$, ft.
(1)	(2)	(3)	(4)	(5)
$CuSO_4$	0.964	0.965	3.8	3.75
$CoSO_4$	0.980	0.977	4.0	3.50

From the K values reported in Tables 2 and 3, separation factors for cobalt sulfate relative to copper sulfate can be computed. From these values in Table 2 (small column data)

$$\alpha = \frac{K_{CoSO_4}}{K_{CuSO_4}} = \frac{0.962}{0.944} = 1.02$$

Separation Plant Requirements

It is important to note that the separation parameters reported above would require extremely large equipment for practical separations. Calculations by Fisher (*16, 21*) indicate that in order to change the ratio of cobalt sulfate to copper sulfate concentrations by a factor of 10, a mass transfer area of 3×10^5 sq.ft./lb. of salt processed per day would be needed. Such a plant would entail a very large capital investment together with significant heat and cooling water requirements and could probably be justified only for a system which was extremely difficult to separate by any other means.

Discrepancies in Results

The lack of agreement between experimental values of K and h_L and those calculated directly from single-stage data is believed due primarily to undefined effects introduced by the cellophane membrane across the diffusion path. Results presented by Long (*21, 22*) indicate that the presence of such a membrane does not affect the Soret coefficients measured in a single-stage cell. However in a continuous column there is a net flux of material across the membrane, and hence its influence might be much more pronounced than in single-stage cells where measurements are made under conditions of zero net flux. The Equations (39) and (41) used in predicting h_L and K were developed under the somewhat naive assumption that the membrane acted simply as an inert, porous barrier and that Soret coefficients in the membrane pores were the same as in the bulk solution. Further experiments are underway to attempt to define the Soret effect through cellophane membranes more clearly.

CONCLUSIONS

The separation of metallic elements by thermal diffusion of their salts in aqueous solution appears feasible, although not necessarily practical from an economic standpoint. Design equations, based on idealized hydrodynamic

and diffusion models, have been developed for predicting the separation behavior of such systems in a horizontal Jury-Von Halle thermal diffusion column. These equations are successful in predicting the effects of column dimensions and operating conditions on the observed separations and should be suitable for scale-up purposes. However in their present form they do not appear satisfactory for predicting separations in continuous equipment from single-stage thermal diffusion (Soret) data alone. Prior to design of a thermal diffusion process for separation of a specific system, operating data should be obtained from a scale model of the column to be employed.

ACKNOWLEDGMENT

All work described herein was carried out under a research contract with the Chemical Technology Division of the Oak Ridge National Laboratory (operated by the Union Carbide Nuclear Company.) The authors wish to express their gratitude for this support and for permission to publish results of the study.

NOTATION

A = total heat transfer area of Soret cell
$\mathcal{D}$ = coefficient of diffusion, area/time
$\mathcal{D}'$ = coefficient of thermal diffusion, area/time-deg.
D = product withdrawal rate, moles/time
$\vec{J}$ = diffusion flux vector, moles/time-area
J_A = net rate of diffusion, moles/time-area
J_o = diffusion rate through the membrane, moles/time-area
J_r } = diffusion rate in the coordinate direction, moles/time-area (components of the flux vector $\vec{J}$)
K = equilibrium constant, dimensionless
K' = equilibrium constant for the complete mixing model
K'' = equilibrium constant for the laminar flow model
L = average flow rate in the cold-side channel, moles/time
R = reflux ratio, L/D
T = temperature, deg.
ΔT = total temperature drop between the top and bottom walls, deg.
V = average flow rate in the hot-side channel, moles/time
Z = total length of the flow channel, length
a = depth of the channel, length
b = width of the membrane (and channel), length
c = $\sigma\tau a$, dimensionless
c' = $\sigma\tau' a (= -c)$, dimensionless
$f_1(c)$ = function defined by Equation (33)
$f_2(c)$ = function defined by Equation (34)
h_L = height of a transfer unit based on the cold side, length
k_L = mass transfer coefficient based on the cold side, moles/time-area
k'_L = mass transfer coefficient based on the cold side and the complete mixing model, moles/time-area
k''_L = mass transfer coefficient based on the cold side and the laminar flow model, moles/time-area
l = coordinate in the membrane, length
r = coordinate in the direction of diffusion, length, and specifically in the hot-side channel
t = time
v = linear velocity of the fluid, length/time
x = average mole fraction of the diffusing component in the cold-side channel
x^* = equilibrium average mole fraction in the cold-side channel
x_D = mole fraction of solute in product from hot channel
x_L = mole fraction of solute in product from cold channel
y = average mole fraction of the diffusing component in the cold-side channel
z = coordinate length of channel, measured in the direction of flow, length

Greek Letters

α = separation factor of copper sulfate to cobalt sulfate
δ = thickness of the membrane, length
ξ = mole fraction of the diffusing component, and specifically, in the hot-side channel
ξ' = mole fraction of the diffusing component in the cold-side channel
ξ'^* = equilibrium mole fraction in the cold-side channel
ξ_o = mole fraction on the hot surface of the membrane
ξ_o' = mole fraction on the cold surface of the membrane
$\xi_o'^*$ = equilibrium mole fraction on the cold surface of the membrane
$\bar{\xi}_1$ = average concentration on the cold side of the Soret cell
$\bar{\xi}_2$ = average concentration on the hot side of the Soret cell
ρ = molar density, moles/volume
σ = Soret coefficient, $(\text{deg.})^{-1}$
τ = temperature gradient in the hot-side channel, deg./length
τ' = temperature gradient in the cold-side channel, deg./length
τ_M = the negative of the temperature gradient in the membrane, deg./length
ϕ = membrane free area, dimensionless

LITERATURE CITED

1. Powers, J. E., and C. R. Wilke, *A.I.Ch.E. Journal*, **3**, 213-220 (1957).
2. Von Halle, Edward, Ph.D. thesis, Univ. Tenn., Knoxville, Tennessee (1959) (U.S.A.E.C. No. K-1420); paper presented with S. H. Jury at A.I.Ch.E. San Francisco meeting (December, 1959).
3. Soret, C., *Arch. Sci. (Geneva)*, **2**, 48 (1879).
4. Chapman, J., H. J. V. Tyrrell, and P. J. Wilson, *J. Chem. Soc.*, **1957**, 2135-2142 (1957).
5. Chipman, J., *J. Am. Chem. Soc.*, **48**, 2577-2589 (1926).
6. Tanner, C. C., *Trans. Faraday Soc.*, **49**, 611-619 (1953)
7. *Ibid.*, **23**, 75 (1927).
8. Tyrrell, H. J. V., *ibid.*, **52**, 940-948 (1956).
9. Alexander, K. F., *Z. Physik Chem.*, **195**, 175-85 (1950).
10. *Ibid.*, **197**, 233-8 (1951).
11. Chanu, J., and J. Lenoble, *Compt. Rend.*, **241**, 115-7 (1955).
12. ———, *J. Chem. Phys.*, **53**, 309-15 (1956).
13. Hirota, K., *J. Chem. Soc. Japan*, **64**, 112-19 (1943).
14. ———, *J. Chem. Phys.*, **18**, 396-7 (1950).
15. ———, *Bull. Chem. Soc. Japan*, **23**, 107-9 (1950).
16. Fisher, G. T., Ph.D. thesis, Univ. Tenn., Knoxville, Tennessee (1960).
17. Bosanquet, L. P., M.S. thesis, Univ. Tenn., Knoxville, Tennessee (1960).
18. Grew, K. E., and T. L. Ibbs, "Thermal Diffusion in Gases," p. 107-111, Cambridge Press, Cambridge, England (1952).
19. Guthrie, G., J. N. Wilson, and V. Schomaker, *J. Chem. Phys.*, **17**, 310-313 (1948).
20. Couch, C. B., B.S. thesis, Univ. Tenn., Knoxville, Tennessee (1959).
21. Fisher, G. T., and John W. Prados, *Ind. Eng. Chem. Fund.*, **2**, No. 4 (November, 1963).
22. Long, G. W., M.S. thesis, Univ. Tenn., Knoxville, Tennessee (1958).

Manuscript received June 26, 1962; revision received April 24, 1963; paper accepted June 4, 1963. Paper presented at A.I.Ch.E Denver meeting.